MNRAS 000, 1–9 (2017) Preprint 18 April 2017 Compiled using MNRAS LATEX style file v3.0

Can Isolated Single Black Holes Produce X-ray Novae?

Tatsuya Matsumoto,[1]⋆ Yuto Teraki,[2,3] and Kunihito Ioka[2]
[1]Department of Physics, Graduate School of Science, Kyoto University, Kyoto 606-8502, Japan
[2]Center for Gravitational Physics, Yukawa Institute for Theoretical Physics, Kyoto University, Kyoto 606-8502, Japan
[3]National Institute of Technology, Asahikawa College, Asahikawa 071-8142, Japan

arXiv:1704.05047v1 [astro-ph.HE] 17 Apr 2017

Accepted XXX. Received YYY; in original form ZZZ

ABSTRACT

Almost all black holes (BHs) and BH candidates in our Galaxy have been discovered as soft X-ray transients, so-called X-ray novae. X-ray novae are usually considered to arise from binary systems. Here we propose that X-ray novae are also caused by isolated single BHs. We calculate the distribution of the accretion rate from interstellar matter to isolated BHs, and find that BHs in molecular clouds satisfy the condition of the hydrogen-ionization disk instability, which results in X-ray novae. The estimated event rate is consistent with the observed one. Possible candidates include *IGR J17454-2919*, *XTE J1908-094*, and *SAX J1711.6-3808*. Near infrared photometric and spectroscopic follow-ups can exclude companion stars for a BH census in our Galaxy.

Key words: black hole physics – stars: black holes – ISM: clouds – X-rays: stars

1 INTRODUCTION

X-ray novae are soft X-ray transient events with a few days of rapid brightening up to $\sim 10^{38}\,\mathrm{erg\,s^{-1}}$, followed by exponential decays (see Tanaka & Shibazaki 1996, for a review). X-ray novae are considered to be produced by binary systems composed of low mass stars and compact objects such as neutron stars or black holes (BHs), so-called a low mass X-ray binary (LMXB) system. About twenty LMXBs have been dynamically confirmed to contain BHs through spectral observations of companion stars. Furthermore, 30-40 of X-ray novae share the same X-ray signatures with those of BH LMXB systems, but they are too faint after an outburst to conduct follow-up observations (Corral-Santana et al. 2016). Therefore, strictly speaking, it is unclear whether these X-ray novae without follow-up observations are really produced by binary systems or not.

In the standard scenario, X-ray novae are explained by the hydrogen-ionization instability of accretion disks (a kind of thermal-viscous instability, see Lasota (2001), for a review). The instability model is originally proposed as a mechanism of dwarf novae, which are optical transients caused by white dwarf binary systems (Osaki 1974; Hōshi 1979), and later applied to X-ray novae (van Paradijs & Verbunt 1984; Cannizzo et al. 1985; Huang & Wheeler 1989; Mineshige & Wheeler 1989). When a region in a disk has low temperature for hydrogen to recombine, the negative hydrogen (H^-) ions dominate the opacity. As opposed to the free-free opacity, the H^- hydrogen opacity is a steep increasing function of temperature. This rapid response to the temperature change makes an S-shaped structure in the thermal equilibrium curve of the region (see Figure 1). In the quiescent phase, the region is in the low temperature branch, while when the surface density reaches a critical value, the region makes a transition to a hot branch and increases the mass accretion rate. Then, the inner annulus is also heated, and the whole disk mass accretes to the central object. This is the origin of X-ray brightening.

Recently, the advanced Laser Interferometer Gravitational Observatory (LIGO) has detected gravitational waves (GWs) and observed binary BH mergers for the first time (Abbott et al. 2016a,c,d). If such merged spinning BHs exist in our Galaxy, they can be high energy sources (Ioka et al. 2016). Before the GW detections, isolated BHs are also believed to reside in our Galaxy. Based on the stellar evolution theory, the number of isolated BHs is as many as $\sim 10^8$ (Shapiro & Teukolsky 1983), some authors have discussed high energy phenomena caused by isolated BHs (Armitage & Natarajan 1999; Barkov et al. 2012; Teraki et al. 2017), and studied the detectability of isolated BHs (Fujita et al. 1998; Agol & Kamionkowski 2002; Fender et al. 2013; Matsumoto et al. 2017). However, because of the very low mass accretion rate, the accretion disks around BHs are radiatively inefficient (Narayan & Yi 1994) and the detection of isolated BHs is challenging if BHs are stationary sources.

In this paper, we propose a novel idea that isolated single BHs in our Galaxy can produce transient events like X-ray novae. The structure of this paper is as follows. First, we calculate the mass accretion distribution of isolated BHs (section 2). Next, we find that some BHs in molecular

⋆ E-mail: matsumoto@tap.scphys.kyoto-u.ac.jp

© 2017 The Authors

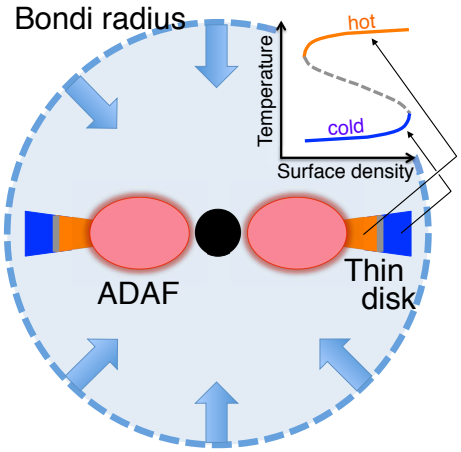

Figure 1. Schematic picture of an isolated BH with a thin disk part attached to inner ADAF part. The thin disk part consists of an outer cold branch and an inner hot branch in the S-shaped thermal equilibrium curve (upper right).

clouds accrete enough mass to have a thin disk part in section 3. This is because for a large mass accretion rate, a disk has a high density enough to cool by radiation and become geometrically thin at the outer part of the disk (Abramowicz et al. 1995; Narayan & Yi 1995). In Figure 1, we show a schematic picture of the system we consider. The thin disk region can suffer from the hydrogen-ionization instability and cause transient events like X-ray novae. We also estimate that the event rate is comparable to that of the observed X-ray novae. Finally, we suggest that some X-ray novae without companions could be produced by isolated BHs in section 4. We also discuss how to discriminate an isolated BH from a binary by observations.

2 ACCRETION RATE DISTRIBUTION OF ISOLATED BHS

In this section, we consider the mass accretion onto Galactic isolated BHs. The BHs accrete interstellar medium (ISM) gas and form accretion disks. We study the accretion rate distribution of isolated BHs taking the BH mass, the BH velocity, and the ISM density distributions into account.

An isolated BH pulls the ISM gas by its gravity and accretes the gas via so-called Bondi accretion (Hoyle & Lyttleton 1939; Bondi & Hoyle 1944; Bondi 1952). The Bondi radius and the accretion rate are estimated as

$$R_{\rm B} = \frac{GM}{c_{\rm s}^2+v^2} \quad (1)$$

$$\simeq 8.3\times10^{13}\left(\frac{M}{10\,{\rm M}_\odot}\right)\left(\frac{V}{40\,{\rm km\,s^{-1}}}\right)^{-2}{\rm cm}, \quad (2)$$

$$\dot{M}_{\rm B} = 4\pi {R_{\rm B}}^2 \rho V \quad (3)$$

$$\simeq 8.2\times10^{11}\left(\frac{M}{10\,{\rm M}_\odot}\right)^{2}\left(\frac{V}{40\,{\rm km\,s^{-1}}}\right)^{-3}\left(\frac{n}{1\,{\rm cm^{-3}}}\right){\rm g\,s^{-1}}, \quad (4)$$

where, G, M, v, $c_{\rm s}$, and ρ are the gravitational constant, the BH mass, the BH velocity, the sound speed of ISM, and the mass density of ISM, respectively. We define the velocity V as $V := \sqrt{c_{\rm s}^2+v^2}$. From Eq. (3) to Eq. (4), we convert the mass density to the number density n by using the relation $\rho = m_{\rm u}\mu n$, where $m_{\rm u}$ and $\mu = 1.41$ are the atomic mass unit and the mean molecular weight. It should be noted that the Bondi accretion rate is much smaller than the Eddington accretion rate defined as

$$\dot{M}_{\rm Edd} = \frac{4\pi G M m_{\rm p}}{\eta\sigma_{\rm T}c} \quad (5)$$

$$\simeq 1.4\times10^{19}\left(\frac{M}{10\,{\rm M}_\odot}\right){\rm g\,s^{-1}}, \quad (6)$$

where $m_{\rm p}$, $\eta = 0.1$, $\sigma_{\rm T}$ and c are the proton mass, radiative efficiency[1], Thomson cross section, and the speed of light, respectively.

The accreting matter forms an accretion disk at the centrifugal radius (Shapiro & Lightman 1976). In the Bondi accretion, the accreting gas is assumed to have a spherical or axial symmetry. However, the actual ISM has density fluctuations. Because of the difference of the density in the scale of the Bondi radius, the accreting ISM has a specific angular momentum of

$$l = \frac{1}{4}\left.\frac{\delta\rho}{\rho}\right|_{R=2R_{\rm B}} R_{\rm B}V. \quad (7)$$

Then, at the centrifugal radius, the gas starts to circulate and forms an accretion disk. The disk size is evaluated by the centrifugal radius as

$$R_{\rm d} := \frac{l^2}{GM} \quad (8)$$

$$\simeq 4.7\times10^{9}\left(\frac{M}{10\,{\rm M}_\odot}\right)^{5/3}\left(\frac{V}{40\,{\rm km\,s^{-1}}}\right)^{-10/3}{\rm cm}. \quad (9)$$

In the second equality, we use the observed density fluctuation in ISM as $\delta\rho/\rho = (R/6\times10^{18}\,{\rm cm})^{1/3}$ (Armstrong et al. 1995; Draine 2011). Since the mass accretion rate is much smaller than the Eddington rate, the accretion disk cools with not radiation but advection, so-called advection dominated accretion flow (ADAF, Narayan & Yi 1994).

For a stationary accretion disk to exist, the infall time at the Bondi radius $t_{\rm fall} := \sqrt{R_{\rm B}^3/GM}$ should be shorter than the dynamical time of a BH to cross the Bondi radius $t_{\rm dyn} := 2R_{\rm B}/v$. This condition is achieved as $t_{\rm fall}/t_{\rm dyn} = v/2V \simeq 0.35 \lesssim 1$, where we set the BH velocity is equal to the sound velocity $v \simeq c_{\rm s}$.

We calculate the mass accretion distribution function of Galactic isolated BHs. The accreting ISM gas has several phases with different densities. BHs also have velocity and mass distributions. Therefore, we have to take into account for these statistical properties. By using the normalized mass and accretion rate defined as $m := M/{\rm M}_\odot$ and $\dot{m} := \dot{M}/\dot{M}_{\rm Edd}$, the mass accretion distribution is given by (Agol & Kamionkowski 2002; Ioka et al. 2016)

$$\frac{dN}{d\dot{m}} = N\int dm\frac{dp(m)}{dm}\int dv\frac{df(v)}{dv}\int dn\frac{d\xi(n)}{dn}h(m,v)\delta\Big(\dot{m}(n,m,v)-\dot{m}\Big), \quad (10)$$

where N, $dp(m)/dm$, $df(v)/dv$, $d\xi(n)/dn$, and $h(m,v)$ are the

[1] Some literatures define the Eddington accretion rate without the radiative efficiency η. It should also be noted that the name "radiative efficiency" does not mean the true efficiency.

total isolated BH number, the BH mass, the BH velocity and the ISM density distribution functions, and a correction factor due to the scale height of the ISM phase and the BH distribution. We set the total number as $N = 10^8$ (Shapiro & Teukolsky 1983). We can integrate Eq. (10) over v and obtain

$$\frac{dN}{d\dot{m}} = N \int dm \frac{dp(m)}{dm} \int dn \frac{df(v_0)}{dv} \frac{d\xi(n)}{dn} h(m, v_0) \frac{V^2|_{v=v_0}}{3v_0\dot{m}}, \quad (11)$$

where v_0 is given by

$$v_0^2 = \left(\frac{GMc\eta\sigma_T\mu n}{\dot{m}}\right)^{2/3} - c_s^2. \quad (12)$$

We briefly explain the BH mass, the BH velocity, and the ISM density distribution functions. These functions are the same as those used in Ioka et al. (2016). For the BH mass distribution function, we assume a Salpeter-like mass function as,

$$\frac{dp(m)}{dm} = Cm^{-\gamma}, \quad (m_{\rm min} < m < m_{\rm max}), \quad (13)$$

where $\gamma = 2.35$ and we normalize the mass function as $\int dm \frac{dp}{dm} = 1$ by setting $C = (\gamma - 1)/(m_{\rm min}^{1-\gamma} - m_{\rm max}^{1-\gamma})$. We set the upper and lower mass as $m_{\rm min} = 5\,{\rm M}_\odot$ and $m_{\rm max} = 15\,{\rm M}_\odot$. The maximum BH mass is motivated by the stellar evolution calculation for the solar abundance (Belczynski et al. 2010). It should be noted that more massive BHs of $\sim 50\,{\rm M}_\odot$ could form in low metallicity environments, as suggested by the GW observations (Abbott et al. 2016b). The number of the massive population could be comparable to that for the solar abundance because the duration of the low metal era is about tenth of the cosmic time, but the star formation rate is also ten times larger than now (Snaith et al. 2014; Haywood et al. 2016). Although considering their contribution is interesting, we do not take them into account because our result does not depend on the maximum BH mass so much.

In this work, we assume a Maxwellian velocity distribution as,

$$\frac{df(v)}{dv} = \sqrt{\frac{2}{\pi}} \frac{v^2}{\sigma_v^3} \exp\left(-\frac{v^2}{2\sigma_v^2}\right), \quad (14)$$

where σ_v is the velocity dispersion. We set this value as $\sigma_v = 40\,{\rm km/s}$. This is motivated by the observed scale height of low mass X-ray binaries from the Galactic plane (White & van Paradijs 1996). Recently, Repetto et al. (2012) have suggested that BHs also receives natal kicks at births and the kick velocity can be the same as those received by neutron stars ($\sim 200 - 400\,{\rm km\,s^{-1}}$). They also used the distance of the binaries from the Galactic plane to deduce the conclusion. However, it should be noted that these arguments depend sensitively on the errors in the evaluated distances. In order to get reliable distance or velocity values, we need more precise measurements such as astrometric observations (Miller-Jones 2014). Such astrometric observations have been applied only for one BH X-ray binary system, Cyg X-1, which has a low proper velocity as $\sim 20\,{\rm km\,s^{-1}}$ (Chevalier & Ilovaisky 1998; Mirabel & Rodrigues 2003; Reid et al. 2011).

We consider five types of the ISM phase: molecular clouds, cold $\rm H_I$, warm $\rm H_I$, warm $\rm H_{II}$, and hot $\rm H_{II}$ mediums. For molecular clouds and cold $\rm H_I$ medium, we adopt the power law distribution as (Berkhuijsen 1999),

$$\frac{d\xi(n)}{dn} = D\xi_0 n^{-\beta}, \quad (n_1 < n < n_2). \quad (15)$$

We normalize the function as $\int dn \frac{d\xi}{dn} = \xi_0$ by choosing the constant $D = (\beta - 1)/(n_1^{1-\beta} - n_2^{1-\beta})$, where ξ_0 is the volume filling factor of the phase in the Galactic volume. The power law index β and the upper and lower density n_1 and n_2 are shown in Table 1. For the warm $\rm H_I$, warm $\rm H_{II}$, and hot $\rm H_{II}$ mediums, we do not consider the density distribution but assume a uniform density with their typical values. Then, we use the delta function for these phases as

$$\frac{d\xi(n)}{dn} = \xi_0 \delta(n - n_1). \quad (16)$$

We take the value of the mean molecular weight as $\mu = 2.82$ for the molecular clouds and $\mu = 1.41$ for the other phases with the Milky Way abundance (Kauffmann et al. 2008).

Finally, we explain the correction factor $h(m, v)$. For a given BH velocity, we can evaluate the BH's scale height by assuming the Galactic potential. We use the following simple potential model as,

$$v_z^2 = v^2/3 \quad (17)$$

$$\frac{1}{2}v_z^2 = \Phi[H(v_z)] \quad (18)$$

$$\frac{\Phi(z)}{2\pi G} = K\left(\sqrt{z^2 + Z^2} - Z\right) + Fz^2, \quad (19)$$

where $Z = 180\,{\rm pc}$, $K = 48\,{\rm M_\odot\,pc^{-2}}$, and $F = 0.01\,{\rm M_\odot\,pc^{-3}}$ (Kuijken & Gilmore 1989a,b). When the derived scale height $H(v_z)$ is larger than the scale height of the ISM phase $H_{\rm d}(X)$, we correct the count by multiplying $H_{\rm d}(X)/H(v_z)$. Then, the correction factor is given by

$$h(m, v) = \min\left[1, \frac{H_{\rm d}(X)}{H(v_z)}\right]. \quad (20)$$

We compile the distribution functions discussed above, and integrate Eq. (11) numerically. In Fig 2, we show the mass accretion distribution of Galactic isolated BHs. The vertical and horizontal axises show the number of BHs and the normalized mass accretion rate, respectively. The normalized accretion rate relates with the BH mass, the BH velocity, and the ISM density as

$$\dot{m} \simeq 5.8 \times 10^{-8} \left(\frac{M}{10\,{\rm M_\odot}}\right)\left(\frac{V}{40\,{\rm km\,s^{-1}}}\right)^{-3}\left(\frac{n}{1\,{\rm cm^{-3}}}\right), \quad (21)$$

where we use Eqs. (3) and (5). The orange-red, dark-blue, magenta, light-green, and turquoise curves show the number distributions of isolated BHs in the molecular clouds, cold $\rm H_I$, warm $\rm H_I$, warm $\rm H_{II}$, and hot $\rm H_{II}$ mediums, respectively.

Let us discuss the shape of the distribution functions in Fig 2. The peak value of the distribution in each ISM medium is roughly evaluated by $N_{\rm peak} \sim N\xi_0 h$. For the hot $\rm H_{II}$ medium, the distribution shows a peaky shape. This is because the hot $\rm H_{II}$ medium has a larger sound velocity c_s than the typical BH velocity $v \sim \sigma_v$, and the distribution reflects only the BH mass distribution. According to the Galactic potential (19), the BH scale height with the velocity $v \sim \sigma_v = 40\,{\rm km\,s^{-1}}$ is estimated as $H(v_z) \simeq 0.3\,{\rm kpc}$. On the other hand, the scale height of the hot $\rm H_{II}$ medium is larger

Table 1. The parameters for each ISM phase. For molecular clouds and cold H_I medium which have broad density distributions, the minimum n_1, maximum n_2 number densities, and power law index of the distributions β are shown. For the other mediums, we show the typical density in the column 2. We represent the volume filling factors ξ_0, the sound velocities c_s, and scale heights H_d in column 5, 6, 7, respectively. For the sound velocity, we include the contribution of the turbulent velocity.

phase	n_1 [cm^{-3}]	n_2 [cm^{-3}]	β	ξ_0	c_s [km s^{-1}]	H_d [kpc]
Molecular cloud	10^2	10^5	2.8	10^{-3}	10	0.075
Cold H_I	10	10^2	3.8	0.04	10	0.15
Warm H_I	0.3	-	-	0.35	10	0.5
Warm H_{II}	0.15	-	-	0.2	10	1
Hot H_{II}	0.002	-	-	0.4	150	3

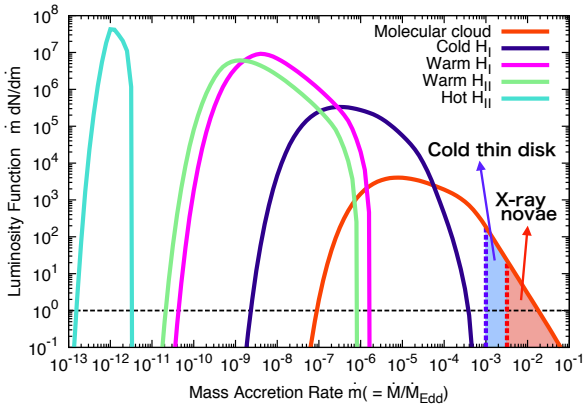

Figure 2. The distribution of the normalized mass accretion rate $\dot{m}$. Each curve shows the accretion distribution in each medium. The orange-red, dark-blue, magenta, light-green, and turquoise solid curves show the number distribution of isolated BHs in the molecular clouds, cold H_I, warm H_I, warm H_{II}, and hot H_{II} mediums, respectively. The red and blue dashed lines represent the critical accretion rates required to produce X-ray novae (Eq. 44, for $m = 15$) and to have a standard disk part (Eq. 29, for $m = 15$ and $n = 10^2$ cm^{-3}), respectively.

than the BH scale height (see Table 1), and the correction factor reduces to unity $h = 1$. Then, the peak value of the distribution of the hot H_{II} medium is given as $N_{peak} \sim 4 \times 10^7\,(N/10^8)(\xi_0/0.4)(h/1)$.

For the warm H_I and H_{II} mediums, the mass accretion distributions have a broader shape than that of the hot H_{II} medium because the sound velocities of these mediums are as large as that of the BH velocity, $c_s \lesssim v \sim \sigma_v$. Therefore, the broadness reflects the velocity distribution. These mediums also have larger scale heights than the BH scale height, and have no correction ($h \sim 1$). However, due to the large dispersion, the peak values of the distributions are a bit smaller than the values estimated by $\sim N\xi_0$.

The accretion distributions of the molecular clouds and the cold H_I medium show tails extending to the large accretion rate ($\dot{m} \gtrsim 10^{-5}$ and 10^{-3}, for the cold H_I medium and the molecular clouds, respectively). These tails are attributed to the density distribution. To estimate the peak values of the distributions, we should take the correction factor h into account, because the molecular clouds and the cold H_I medium have smaller scale heights than that of BHs, $H_d(X) < H(v_z)$, which requires corrections of $h \sim 0.1 - 0.3$.

3 X-RAY NOVAE PRODUCED BY ISOLATED BHS

We discuss the possibility that isolated BHs produce X-ray transient events, such as X-ray novae. In section 2, we consider that the accretion disks formed around isolated BHs are ADAFs. However, when the accretion rate is larger than a critical value, the radiative cooling overcomes the advective one and the ADAF becomes a standard disk (Abramowicz et al. 1995). Furthermore, if the standard disk has a low temperature region enough to allow hydrogen to recombine, the disk suffers from the hydrogen-ionization instability and produces an X-ray transient event.

When the mass accretion rate is large, an ADAF can accompany a standard disk at the outer part of the disk. This is because at a large radius from the central BH, the radiative cooling rate gets comparable to the advective cooling and viscosity heating rates. We can see this easily by considering the energy equation of ADAFs as

$$(1 - f)q_{vis} \simeq q_{bre}, \tag{22}$$

where q_{vis} and q_{bre} are the viscous heating and the bremsstrahlung cooling rates per volume, respectively. We also assume that the advective cooling rate is approximately given by the viscous heating rate as $q_{adv} \simeq f q_{vis}$, where f is the efficiency parameter and we set $f = 0.5$ for a fiducial value at the transition region to a standard disk (Narayan & Yi 1995). Then, the left hand side of Eq. (22) represents a net heating rate. By using a self-similar solution of ADAF, we can show that the heating rate depends on radius r as $q_{vis} \propto r^{-4}$ (Narayan & Yi 1994, 1995), where we normalize a radius by the Schwarzschild radius $R_S = 2GM/c^2$ as $r := R/R_S$. The bremsstrahlung cooling rate is given by Svensson (1982), and we can show the radius dependence of the cooling rate as $q_{bre} \propto r^{-7/2}$, where we use the ADAF self-similar solution and assume that electrons have a non-relativistic virial temperature of ions[2] as (Narayan & Yi 1995; Matsumoto et al. 2017)

$$T_e \simeq 3.2 \times 10^{12}\,\beta_{ADAF}\,c_3\,r^{-1}\,\mathrm{K}. \tag{23}$$

The constants β_{ADAF} and c_3 are the parameters of the ADAF self-similar solution (see below Eq. (25) for more detailed explanation). Then, at a large radius, the radiative cooling rate becomes comparable to the viscous heating rate, and the ADAF becomes a standard disk. Equation (22) is rewritten

[2] At the outer part of the ADAF ($r \gtrsim 100$), the Coulomb collision works well and makes the electron temperature equal to the ion temperature.

to the condition for the critical accretion rate at a given radius by using the self-similar solution as (Abramowicz et al. 1995; Narayan & Yi 1995),

$$\dot{m}_{\rm crit} \simeq 2.3\left(\frac{m_{\rm u}}{m_{\rm e}}\right)^{1/2}\frac{\eta}{\alpha_{\rm f}}\,\epsilon'(1-f)c_1^2c_3\alpha^2\beta_{\rm ADAF}^{-1/2}r^{-1/2} \quad (24)$$

$$\simeq 1.4\times10^3\,\epsilon'(1-f)c_1^2c_3\alpha^2\beta_{\rm ADAF}^{-1/2}r^{-1/2} \quad (25)$$

$$\simeq 4.4\times10^{-1}\left(\frac{\epsilon'}{0.63}\right)\left(\frac{1-f}{0.5}\right)\left(\frac{c_1}{0.48}\right)^2\left(\frac{c_3}{0.32}\right)\left(\frac{\alpha}{0.1}\right)^2\left(\frac{\beta_{\rm ADAF}}{0.5}\right)^{-1/2}r^{-1/2}, \quad (26)$$

where $m_{\rm e}$, $\alpha_{\rm f}$, α and $\beta_{\rm ADAF}$ are the electron mass, the fine structure constant, the viscosity parameter (Shakura & Sunyaev 1973) and the ratio of the gas pressure to the total pressure, respectively. For fiducial values, we set $\alpha = 0.1$ and $\beta_{\rm ADAF} = 0.5$. The constants ϵ', c_1, and c_3 appear in the derivation of the ADAF self-similar solution as functions of f, α, and $\beta_{\rm ADAF}$ (Narayan & Yi 1994, 1995). The notation of these constants is the same as given in Narayan & Yi (1994, 1995), except for $\beta_{\rm ADAF}$ (where $\beta_{\rm ADAF}$ is written as β).

If $\dot{m} \gtrsim \dot{m}_{\rm crit}$, the radiative cooling overcomes the advective cooling and no longer the ADAF part exists. Observations of BH X-ray binaries also suggest an outer standard accretion disk truncated in the inner part by radiatively inefficient accretion flow, which can explain some properties of BH X-ray binaries such as the spectral transition between the high-soft state and the low-hard state (Esin et al. 1997; Lasota 2001; Done et al. 2007).

We estimate how many isolated BHs have the standard disk part. We define the transition radius $r_{\rm tr}(= R_{\rm tr}/R_{\rm S})$ by $\dot{m} = \dot{m}_{\rm crit}(r = r_{\rm tr})$, where the ADAF part begins to cool radiatively and makes a transition to the standard disk outer-part. By using Eqs. (21) and (25), we obtain the transition radius as,

$$r_{\rm tr} \simeq 1.5\times10^9\left(\frac{m}{10}\right)^{-2}\left(\frac{V}{40\,{\rm km\,s^{-1}}}\right)^6\left(\frac{n}{10^2\,{\rm cm^{-3}}}\right)^{-2}. \quad (27)$$

It should be noted that when we discuss the BHs in molecular clouds, we should use the mean molecular weight of $\mu = 2.82$ in Eq. (21). We use the fiducial values for the ADAF parameters in Eq. (25). In the following, we also use the fiducial values and do not show the dependences of ADAF parameters explicitly. For a disk to have a standard disk part, the transition radius should be smaller than the disk radius $r_{\rm d} := R_{\rm d}/R_{\rm S}$. With Eq. (8), this condition is rewritten to a condition for the velocity V as,

$$V \lesssim 9.2\left(\frac{m}{10}\right)^{2/7}\left(\frac{n}{10^2\,{\rm cm^{-3}}}\right)^{3/14}{\rm km\,s^{-1}}. \quad (28)$$

Since the velocity is $V > c_{\rm s} = 10\,{\rm km\,s^{-1}}$, to satisfy the above condition, the BH mass and the density should be larger than the minimum values, $m > 5$ and $n > 10^2\,{\rm cm^{-3}}$. Hereafter, we use $m = 15$ for the fiducial value. By substituting Eq. (28) into Eq. (21), we obtain a required minimum accretion rate for an isolated BH to have a standard disk part as

$$\dot{m} \gtrsim \dot{m}_{\rm disk} = 1.0\times10^{-3}\left(\frac{m}{15}\right)^{1/7}\left(\frac{n}{10^2\,{\rm cm^{-3}}}\right)^{5/14}\left(\frac{\epsilon'}{0.63}\right)^{9/14}\left(\frac{1-f}{0.5}\right)^{9/14}\left(\frac{c_1}{0.48}\right)^{9/7}\left(\frac{c_3}{0.32}\right)^{9/14}\left(\frac{\alpha}{0.1}\right)^{9/7}\left(\frac{\beta_{\rm ADAF}}{0.5}\right)^{-9/28}, \quad (29)$$

where we restore the ADAF parameter dependences. In Fig 2, we show the minimum accretion rate with a blue dashed line for $m = 15$ and $n = 10^2\,{\rm cm^{-3}}$.

Next, we discuss the possibility that hydrogen recombines in the thin disk part. We firstly compare the recombination temperature with the temperature in the disk for simplicity, and later discuss the details. The Saha equation gives the hydrogen recombination temperature in the thin disk. When hydrogen is partially ionized, their ionization state determines the abundance of H^- ion (i.e., opacity) (The metal abundance may not change results so much as long as hydrogen mainly supplies electrons). The Saha equation gives the ratio of the ionized hydrogen number density $n_{\rm H^+}$ to the neutral hydrogen density $n_{\rm H}$ as

$$\frac{n_{\rm H^+}n_{\rm e}}{n_{\rm H}} = \frac{(2\pi m_{\rm e}k_{\rm B}T)^{3/2}}{h^3}\exp\left(-\frac{\chi_{\rm H}}{k_{\rm B}T}\right), \quad (30)$$

where $n_{\rm e}$, $k_{\rm B}$, h, and $\chi_{\rm H} = 13.6\,{\rm eV}$ are the electron number density, the Boltzmann constant, the Planck constant, and the hydrogen ionization energy. With the definition of the degree of ionization $x := n_{\rm e}/(n_{\rm H} + n_{\rm H^+})$, and the charge neutrality $n_{\rm e} = n_{\rm H^+}$, Eq. (30) is rewritten as

$$\frac{x^2}{1-x} = \frac{(2\pi m_{\rm e}k_{\rm B}T)^{3/2}}{n_{\rm H,tot}h^3}\exp\left(-\frac{\chi_{\rm H}}{k_{\rm B}T}\right), \quad (31)$$

where $n_{\rm H,tot} = n_{\rm H} + n_{\rm H^+}$ is the total number density of hydrogen. We simply define the partially ionized state of the hydrogen as $x = 0.5$, which results in the value of the right hand side of Eq. (31) of 0.5. The temperature and the mass density are given by formulae of the standard disk with gas pressure and free-free absorption (Shakura & Sunyaev 1973; Kato et al. 2008) as

$$T = 1.4\times10^8\,\alpha^{-1/5}\,m^{-1/5}\,\dot{m}^{3/10}\,r^{-3/4}\,{\rm K} \quad (32)$$

$$\rho = 1.7\times10^2\,\alpha^{-7/10}\,m^{-7/10}\,\dot{m}^{11/20}\,r^{-15/8}\,{\rm g\,cm^{-3}}. \quad (33)$$

The total number density of hydrogen is obtained by $n_{\rm H,tot} = \rho X/m_{\rm p}$, where $X = 0.7$ is the mass fraction of hydrogen for the solar abundance. Substitution of above expressions for Eq. (31) yields the radius where hydrogen begins to recombine as

$$r \simeq 8.3\times10^3\left(7.4+\ln\left[\alpha^{2/5}m^{2/5}\dot{m}^{-1/10}r^{3/4}\right]\right)^{4/3}\alpha^{-4/15}m^{-4/15}\dot{m}^{2/5} \quad (34)$$

$$\simeq 1.3\times10^4\left(\frac{\alpha}{0.1}\right)^{-4/15}\left(\frac{m}{15}\right)^{-4/15}\left(\frac{\dot{m}}{10^{-3}}\right)^{2/5}. \quad (35)$$

From the first to the second line, we substitute the arguments in the natural logarithm for the typical parameter values $\alpha = 0.1$, $m = 15$, $\dot{m} = 10^{-3}$, and $r = 10^4$ suggested by Eq. (29). The necessary accretion rate for hydrogen recombination is also obtained by solving Eq. (35) for the mass

accretion rate as [3]

$$\dot{m} \simeq 8.0 \times 10^{-15} \left(\frac{\alpha}{0.1}\right)^{2/3} r^{5/2} m^{2/3}. \quad (36)$$

By substituting the above radius into the temperature (32), we obtain

$$T \simeq 1.3 \times 10^4 \,\mathrm{K}. \quad (37)$$

This disk temperature corresponds to the effective temperature of

$$T_{\rm eff} = \left[\frac{3GM\dot{M}}{8\pi\sigma_{\rm SB}R^3}\right]^{1/4} \simeq 4.5 \times 10^3 \left(\frac{\alpha}{0.1}\right)^{1/5} \left(\frac{m}{15}\right)^{-1/20} \left(\frac{\dot{m}}{10^{-3}}\right)^{-1/20} \mathrm{K}, \quad (38)$$

where $\sigma_{\rm SB}$ is the Stefan-Boltzmann constant. The hydrogen recombination temperature (37) should be compared with the temperature of the disks which we consider.

We roughly estimate the temperature of the thin disk part and show that the disk has a low temperature region where hydrogen can recombine. We use the standard disk formulae in eq. (32), and evaluate the disk temperature as

$$T \simeq 2.8 \times 10^3 \left(\frac{m}{15}\right)^{-1/5} \left(\frac{\dot{m}}{10^{-3}}\right)^{10/3} \left(\frac{r_{\rm d}}{10^5}\right)^{-3/4} \left(\frac{\alpha}{0.1}\right)^{-1/5} \mathrm{K}, \quad (39)$$

where we use the accretion rate and the disk radius of $\dot{m} = 10^{-3}$ and $r_{\rm d} = 10^5$ which corresponds to BHs with $m = 15$ and $V = 10\,\mathrm{km\,s^{-1}}$. This value is lower than the hydrogen recombination temperature in Eq. (37). Therefore, the thin disk part of isolated BHs with accretion rate $\dot{m} \gtrsim 10^{-3}$ has the region where hydrogen begins to recombine and makes the disk unstable.

We study the condition of hydrogen recombination more precisely than the above discussion, in particular, on the basis of the disk instability theory (van Paradijs 1996). For an instability to occur, the mass accretion rate should be in the middle branch of the S-curve at some radius. The maximum and minimum accretion rates of the branch are calculated numerically, and fitting formulae are given by Lasota et al. (2008) as

$$\dot{m}^{+}_{\rm crit} = 6.36 \times 10^{-15} \left(\frac{\alpha}{0.1}\right)^{-0.01} r^{2.64} m^{0.75}, \quad (40)$$

$$\dot{m}^{-}_{\rm crit} = 3.91 \times 10^{-15} \left(\frac{\alpha}{0.1}\right)^{0.01} r^{2.58} m^{0.73}, \quad (41)$$

where we rewrite the radius and mass from the original notations in Lasota et al. (2008) to the normalized ones, and keep the viscosity parameter α explicitly. It should be noted the numerically obtained maximum accretion rate (40) is roughly reproduced by our analytical formula (36) except for the dependence on the viscosity parameter α. Since the critical rates are increasing functions of radius, for an unstable annulus to exist, the mass accretion rate should be smaller than the maximum rate (40) at the disk radius, $\dot{m} < \dot{m}^{+}_{\rm crit}(r = r_{\rm d})$, and should also be larger than the minimum rate (41) at the transition radius, $\dot{m} > \dot{m}^{-}_{\rm crit}(r = r_{\rm tr})$. For the first condition, the maximum rate at the disk radius is given by

$$\dot{m}^{+}_{\rm crit}(r = r_{\rm d}) = 5.7 \left(\frac{\alpha}{0.1}\right)^{-0.01} \left(\frac{m}{15}\right)^{2.51} \left(\frac{V}{10\,\mathrm{km\,s^{-1}}}\right)^{-8.8} \quad (42)$$

where we use Eq. (8) for the disk radius. We see that the first condition is easily satisfied. For the second condition, we substitute Eq. (27) to the minimum rate and obtain

$$\dot{m}^{-}_{\rm crit}(r = r_{\rm tr}) = 7.3 \times 10^{-1} \left(\frac{\alpha}{0.1}\right)^{0.01} \left(\frac{m}{15}\right)^{-4.43} \left(\frac{V}{10\,\mathrm{km\,s^{-1}}}\right)^{15.48} \left(\frac{n}{10^2\,\mathrm{cm^{-3}}}\right)^{-5.16}. \quad (43)$$

At first glance, this condition does not seem to be satisfied. However, for BHs with $\dot{m} \gtrsim 10^{-3}$, the density is larger than $n = 10^2\,\mathrm{cm^{-3}}$, which decrease the minimum rate from the above value. More precisely, to satisfy the second condition, an inequality $(m/15)^{0.88}(n/10^2\,\mathrm{cm^{-3}})(V/10\,\mathrm{km\,s^{-1}})^{-3} > 2.9$ should hold. Then, by noting that $\dot{m} \propto mV^{-3}n$, we obtain the condition for isolated BHs to satisfy the second condition

$$\dot{m} \gtrsim \dot{m}_{\rm XRN} \simeq 3.2 \times 10^{-3} \left(\frac{m}{15}\right)^{0.12} \left(\frac{\epsilon'}{0.63}\right)^{0.84} \left(\frac{1-f}{0.5}\right)^{0.84} \left(\frac{c_1}{0.48}\right)^{1.68} \left(\frac{c_3}{0.32}\right)^{0.84} \left(\frac{\alpha}{0.1}\right)^{1.68} \left(\frac{\beta_{\rm ADAF}}{0.5}\right)^{-0.42} \quad (44)$$

where we restore the ADAF parameter dependences. In Fig. 2, we also show the required accretion rate for $m = 15$ with a red dashed line.

We conclude that isolated BHs with a mass accretion rate larger than the critical rates (29) and (44) suffer from the hydrogen-ionization instability and cause transient events such as X-ray novae. In Fig 2, we show the population which causes transients with a red shaded region. We see that the number of the isolated BHs which can produce X-ray novae-like transients by the ionization instability is about $N_{\rm BH} \sim 20$. BHs in a blue shaded region have mass accretion rates of $\dot{m}_{\rm disk} < \dot{m} < \dot{m}^{-}_{\rm crit}(r = r_{\rm tr})$. In this case, the whole region of the thin disk parts is always in the cold branch and stable (Menou et al. 1999).

Finally, we estimate the event rate and show that the rate is consistent with the observations. We assume that, in an outburst phase, the BHs have the same luminosity and duration as the observed X-ray novae of $L_{\rm burst} \sim 0.2 L_{\rm Edd}$ ($\dot{M}_{\rm burst} \sim 0.2\dot{M}_{\rm Edd}$) and $t_{\rm burst} \sim 30\,\mathrm{days}$ (Chen et al. 1997). To power the outbursts, BHs with $\dot{M} \sim 3 \times 10^{-3}\dot{M}_{\rm Edd}$ should continue to accrete mass with a duration of

$$t_{\rm quiet} \sim \frac{t_{\rm burst}\dot{M}_{\rm burst}}{\dot{M}}, \quad (45)$$

$$\sim 2000 \left(\frac{t_{\rm burst}}{30\,\mathrm{d}}\right) \left(\frac{\dot{M}_{\rm burst}}{0.2\,\dot{M}_{\rm Edd}}\right) \left(\frac{\dot{M}}{3 \times 10^{-3}\,\dot{M}_{\rm Edd}}\right)^{-1} \mathrm{days}. \quad (46)$$

It should be noted that the derived duration is less than the dynamical timescale of a BH to cross the Bondi radius $t_{\rm byn}$ for $V = 10\,\mathrm{km\,s^{-1}}$, which corresponds to the angular momentum flip timescale of the disk. Then, the event rate is

[3] When hydrogen recombines and makes the opacity large, convection develops in accretion disks, which decreases the vertical temperature gradient (Meyer & Meyer-Hofmeister 1982; Cannizzo & Wheeler 1984). Therefore, if the convective motion reaches the midplane of the disk, the standard disk formula (32) overestimates the disk temperature. However, Cannizzo & Wheeler (1984) shows that the convection does not reach the midplane at the maximum accretion rate of the S-curve middle branch.

estimated as

$$\frac{N_{\rm BH}}{t_{\rm quiet}} \sim 3.6 \left(\frac{N_{\rm BH}}{20}\right)\left(\frac{t_{\rm burst}}{30\,{\rm d}}\right)^{-1}\left(\frac{\dot{M}_{\rm burst}}{0.2\,\dot{M}_{\rm Edd}}\right)^{-1}\left(\frac{\dot{M}}{3\times10^{-3}\,\dot{M}_{\rm Edd}}\right){\rm yr}^{-1}. \quad (47)$$

Interestingly, this value is comparable to the rate of the observed X-ray novae (∼ a few $\rm yr^{-1}$, Chen et al. 1997; Corral-Santana et al. 2016). Therefore, a fraction of X-ray novae may be produced by isolated BHs. In order to study this possibility, we need deep and multi-wavelength follow-up observations to confirm whether X-ray novae occur in molecular clouds, and whether there are companion stars or not.

4 DISCUSSION

We discuss the observational strategy to confirm whether an X-ray nova is produced by an isolated BH or not. The simplest way is to exclude companion (or secondary) stars by follow-up observation. Typically, secondary stars of low mass BH X-ray binaries are K- or M-type dwarves (Remillard & McClintock 2006). Their effective temperature and radius are about $T_{\rm eff} \sim 4000\,{\rm K}$ and $R_* \sim 0.5\,R_\odot$ (Torres et al. 2010).

Then, we estimate the apparent magnitudes for optical V- ($\lambda_V = 0.545\,\mu$m) and near infrared J- ($\lambda_J = 1.215\,\mu$m), H- ($\lambda_H = 1.654\,\mu$m), and K_s-bands ($\lambda_{K_s} = 2.157\,\mu$m) of the companion stars taking the extinction into account. We set the distance to an isolated BH $d \sim 4\,$kpc, which is a typical distance to dynamically confirmed BHs (Corral-Santana et al. 2016). For this distance, the hydrogen column density contributed from the interstellar space, amounts to $N_{\rm H} \sim 1.2\times10^{22}(n/1\,{\rm cm^{-3}})(d/4\,{\rm kpc})\,{\rm cm^{-2}}$, where n denotes the number density of the interstellar space. On the other hand, the column density of the molecular clouds where the BH resides, is $N_{\rm H} \sim 0.9\times10^{22}(n/10^2\,{\rm cm^{-3}})(l/30\,{\rm pc})\,{\rm cm^{-2}}$, where we use a typical molecular cloud size of $l \sim 30\,$pc (Miville-Deschênes et al. 2017). We see that these contributions are comparable, and we set the total column density as $N_{\rm H} = 2\times10^{22}\,{\rm cm^{-2}}$ to estimate the extinction. For the column density, the extinction of each band results in $A_V \simeq 12\,$mag, $A_J \simeq 3.2\,$mag, $A_H \simeq 2.0\,$mag and $A_{K_s} \simeq 1.4\,$mag, where we use $A_\lambda/N_{\rm H} \simeq 6.0$, 1.6, 1.0, and $0.7\times10^{-22}\,{\rm cm^2}$ mag for V-, J-, H-, and K_s-bands, respectively (Draine 2003). Then, the apparent magnitudes in these bands become $V \simeq 33.6\,$mag, $J \simeq 23.4\,$mag, $H \simeq 22.3\,$mag and $K_s \simeq 21.9\,$mag. We find that optical follow-up observations are extremely difficult to detect secondary stars.

We discuss an observational strategy to confirm the absence of companions in near infrared bands. When an X-ray nova is produced by a binary system, we can find the secondary star by deep near infrared follow-ups. In the actual observations, we can use rough estimations of the column density by using the absorption signature of the soft X-ray spectrum (Liu et al. 2007; Corral-Santana et al. 2016, and references therein), in order to evaluate the necessary depths for follow-ups. In Fig. 3, we show the required depth to detect companion stars if they exists. Some observed X-ray novae whose column densities are evaluated by fitting of the absorbed soft X-ray spectrum (Corral-Santana et al. 2016, and references therein) are also shown. The selected X-ray novae are located at the low galactic latitude position $b \lesssim 1.5\,$deg because their host molecular clouds have small scale heights (see Table 1). Horizontal dotted lines represent the column density of each transient. Red, green, blue, and magenta curves show the estimated apparent AB magnitude, when the companions are located at 4 kpc from Sun, including extinction in $V-$, $J-$, $H-$, and K_s-bands, respectively. For example, *MAXI J1543-564* has a column density of $\simeq 1.4\times10^{22}\,{\rm cm^{-2}}$. With this density, we should conduct follow-up observations as deep as ∼ 22.5, 21.6, and 21.4 mag in J-, H-, K_s-bands. If we can not detect any sources, the transient could be launched by an isolated BH.

It should be also noted that a detection of near infrared sources does not necessarily mean the existence of the companion. We also detect the disk as a near infrared source. In this case, we should conduct spectroscopic observations. When the near infrared source is not the companion but the disk emission of an isolated BH, we do not detect any periodic variation of emission or absorption lines (e.g., $\rm H_I$ and $\rm He_{II}$ emission lines, or neutral metals and molecular absorption lines, as actually observed in BH binary systems Khargharia et al. 2010). In a catalog of BH X-ray novae (Corral-Santana et al. 2016), such near infrared candidate sources without periodic variabilities have been already reported, e.g. *IGR J17454-2919*, *XTE J1908-094*, and *SAX J1711.6-3808*. Among these X-ray novae, *IGR J17454-2919* (Paizis et al. 2015) and *SAX J1711.6-3808* (Wang & Wang 2014) are located at the same positions where the near infrared sources have already been detected in the past survey observations, although the positions are crowded with stars and the chance of coincidence is high. Further follow-up observations are not conducted. For the other X-ray nova, *XTE J1908-094* (Chaty et al. 2006), only photometric observations were conducted, and any detections of periodic variabilities were not reported. We should conduct deeper and more careful photometric and spectroscopic observations for these objects.

Radio follow-up observations are also important to study whether the transients are accompanied by molecular clouds or not. For example, the X-ray source *1E 1740.7-2942* in the Galactic center was first proposed to be in a giant molecular cloud by radio observations (Bally & Leventhal 1991; Mirabel et al. 1991), but later shown to be located behind the cloud by detailed X-ray spectroscopic observations (Churazov et al. 1996).

We also discuss the feedback effect of isolated BHs on the event rate. Theoretical studies suggests that ADAF solutions allow outflows from the disk systems (Blandford & Begelman 1999, 2004; Yuan et al. 2015). Even a small fraction of accretion mass is blown away, the outflow affects the medium around the Bondi radius (Ioka et al. 2016). When the feedback works, the accretion rate is decreased, which also makes the outflows weak. Ioka et al. (2016) estimated the duty cycle of the self-regulation is about ∼ 1/10. In this case, the event rate of X-ray novae produced by isolates BHs will be decreased by ∼ 1/10.

When an X-ray flux from the inner disk part is large, it may affect the disk structure (van Paradijs 1996). The X-rays ionize hydrogen and the Saha equation (30) does not give a correct degree of ionization. Dubus et al. (1999) studied the effect of the X-ray irradiation and concluded that the disk structure nor the S-curve do not change so much in the quiescent state. However, if the accretion disk is warped or

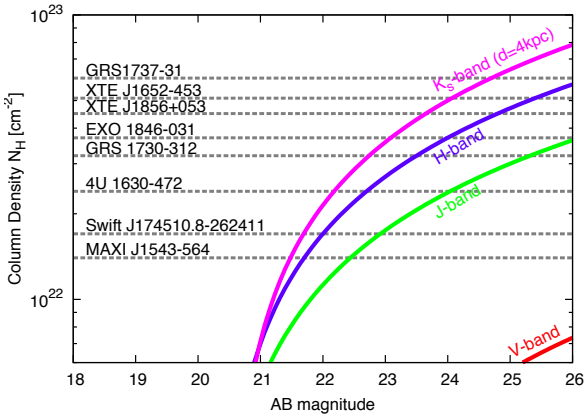

Figure 3. The required depth to detect the companion stars of the observed X-ray novae with the measured column densities. Red, green, blue, and magenta curves show the apparent magnitude of the companion stars, when the companions whose temperature and photospheric radius of $T_{\rm eff} \sim 4000\,{\rm K}$ and $R_* \sim 0.5\,R_\odot$, are located at 4 kpc from Sun. The horizontal dotted lines represent the measured column densities for X-ray novae which are not confirmed to have companions.

there is a X-ray irradiation source above the disk plane, the X-ray ionization may affect the hot branch in the S-curve. This is an interesting future work.

Finally, we remark the difference between our work and Agol & Kamionkowski (2002) who also discussed a probability that isolated BHs launches X-ray novae. They calculated the event rate of X-ray novae produced by isolated BHs by using the mass accretion distribution. Their calculation predicted much more event rate than the observed one, and they concluded that X-ray novae caused by isolated BHs are unlikely. However, they did not consider the disk structure and the instability condition, and extremely underestimate the minimum accretion rate needed to produce X-ray novae. This is why Agol & Kamionkowski (2002) overestimated the event rate of X-ray novae powered by isolated BHs.

ACKNOWLEDGEMENTS

We are thankful Aya Bamba and Shota Kisaka for fruitful discussions and comments. We also would like to thank Hitoshi Negoro for carefully reading the manuscript and giving us useful comments. T.M. is especially thankful to Takashi Hosokawa for helpful discussions and daily encouragements. This work is supported by KAKENHI 24000004, 24103006, 26247042, 26287051, and 17H01126 (K.I.). T. M. will also be supported by the Grants-in-Aid for the Japan Society for the Promotion of Science (JSPS) Fellows.

REFERENCES

Abbott, B. P., Abbott, R., Abbott, T. D., et al. 2016, Physical Review Letters, 116, 061102
Abbott, B. P., Abbott, R., Abbott, T. D., et al. 2016, ApJ, 818, L22
Abbott, B. P., Abbott, R., Abbott, T. D., et al. 2016, Physical Review Letters, 116, 241103
Abbott, B. P., Abbott, R., Abbott, T. D., et al. 2016, Physical Review X, 6, 041015
Abramowicz, M. A., Chen, X., Kato, S., Lasota, J.-P., & Regev, O. 1995, ApJ, 438, L37
Agol, E., & Kamionkowski, M. 2002, MNRAS, 334, 553
Armitage, P. J., & Natarajan, P. 1999, ApJ, 523, L7
Armstrong, J. W., Rickett, B. J., & Spangler, S. R. 1995, ApJ, 443, 209
Bally, J., & Leventhal, M. 1991, Nature, 353, 234
Barkov, M. V., Khangulyan, D. V., & Popov, S. B. 2012, MNRAS, 427, 589
Blandford, R. D., & Begelman, M. C. 1999, MNRAS, 303, L1
Blandford, R. D., & Begelman, M. C. 2004, MNRAS, 349, 68
Belczynski, K., Bulik, T., Fryer, C. L., et al. 2010, ApJ, 714, 1217
Berkhuijsen, E. M. 1999, Plasma Turbulence and Energetic Particles in Astrophysics, 61
Bondi, H., & Hoyle, F. 1944, MNRAS, 104, 273
Bondi, H. 1952, MNRAS, 112, 195
Cannizzo, J. K., Wheeler, J. C., & Ghosh, P. 1985, Cataclysmic Variables and Low-Mass X-ray Binaries, 113, 307
Cannizzo, J. K., & Wheeler, J. C. 1984, ApJS, 55, 367
Chaty, S., Mignani, R. P., & Israel, G. L. 2006, MNRAS, 365, 1387
Chen, W., Shrader, C. R., & Livio, M. 1997, ApJ, 491, 312
Chevalier, C., & Ilovaisky, S. A. 1998, A&A, 330, 201
Churazov, E., Gilfanov, M., & Sunyaev, R. 1996, ApJ, 464, L71
Corral-Santana, J. M., Casares, J., Muñoz-Darias, T., et al. 2016, A&A, 587, A61
Done, C., Gierliński, M., & Kubota, A. 2007, A&ARv, 15, 1
Draine, B. T. 2003, ARA&A, 41, 241
Draine, B. T. 2011, Physics of the Interstellar and Intergalactic Medium by Bruce T. Draine. Princeton University Press, 2011. ISBN: 978-0-691-12214-4,
Dubus, G., Lasota, J.-P., Hameury, J.-M., & Charles, P. 1999, MNRAS, 303, 139
Esin, A. A., McClintock, J. E., & Narayan, R. 1997, ApJ, 489, 865
Fender, R. P., Maccarone, T. J., & Heywood, I. 2013, MNRAS, 430, 1538
Fujita, Y., Inoue, S., Nakamura, T., Manmoto, T., & Nakamura, K. E. 1998, ApJ, 495, L85
Haywood, M., Lehnert, M. D., Di Matteo, P., et al. 2016, A&A, 589, A66
Hōshi, R. 1979, Progress of Theoretical Physics, 61, 1307
Hoyle, F., & Lyttleton, R. A. 1939, Proceedings of the Cambridge Philosophical Society, 35, 405
Huang, M., & Wheeler, J. C. 1989, ApJ, 343, 229
Ioka, K., Matsumoto, T., Teraki, Y., Kashiyama, K., & Murase, K. 2016, arXiv:1612.03913
Kato, S., Fukue, J., & Mineshige, S. 2008, Black-Hole Accretion Disks — Towards a New Paradigm —, 549 pages, including 12 Chapters, 9 Appendices, ISBN 978-4-87698-740-5, Kyoto University Press (Kyoto, Japan), 2008.,
Kauffmann, J., Bertoldi, F., Bourke, T. L., Evans, N. J., II, & Lee, C. W. 2008, A&A, 487, 993
Khargharia, J., Froning, C. S., & Robinson, E. L. 2010, ApJ, 716, 1105
Kuijken, K., & Gilmore, G. 1989, MNRAS, 239, 571
Kuijken, K., & Gilmore, G. 1989, MNRAS, 239, 605
Lasota, J.-P. 2001, New Astron. Rev., 45, 449
Lasota, J.-P., Dubus, G., & Kruk, K. 2008, A&A, 486, 523
Liu, Q. Z., van Paradijs, J., & van den Heuvel, E. P. J. 2007, A&A, 469, 807
Matsumoto, T., Teraki, Y., & Ioka, K. 2017, in prep
Menou, K., Narayan, R., & Lasota, J.-P. 1999, ApJ, 513, 811
Meyer, F., & Meyer-Hofmeister, E. 1982, A&A, 106, 34
Miller-Jones, J. C. A. 2014, Publ. Astron. Soc. Australia, 31, e016
Mineshige, S., & Wheeler, J. C. 1989, ApJ, 343, 241

Mirabel, I. F., Paul, J., Cordier, B., Morris, M., & Wink, J. 1991, A&A, 251, L43
Mirabel, I. F., & Rodrigues, I. 2003, Science, 300, 1119
Miville-Deschênes, M.-A., Murray, N., & Lee, E. J. 2017, ApJ, 834, 57
Narayan, R., & Yi, I. 1994, ApJ, 428, L13
Narayan, R., & Yi, I. 1995, ApJ, 452, 710
Osaki, Y. 1974, PASJ, 26, 429
Paizis, A., Nowak, M. A., Rodriguez, J., et al. 2015, ApJ, 808, 34
van Paradijs, J., & Verbunt, F. 1984, American Institute of Physics Conference Series, 115, 49
van Paradijs, J. 1996, ApJ, 464, L139
Remillard, R. A., & McClintock, J. E. 2006, ARA&A, 44, 49
Repetto, S., Davies, M. B., & Sigurdsson, S. 2012, MNRAS, 425, 2799
Reid, M. J., McClintock, J. E., Narayan, R., et al. 2011, ApJ, 742, 83
Shakura, N. I., & Sunyaev, R. A. 1973, A&A, 24, 337
Shapiro, S. L., & Lightman, A. P. 1976, ApJ, 204, 555
Shapiro, S. L., & Teukolsky, S. A. 1983, Research supported by the National Science Foundation. New York, Wiley-Interscience, 1983, 663 p.,
Snaith, O. N., Haywood, M., Di Matteo, P., et al. 2014, ApJ, 781, L31
Svensson, R. 1982, ApJ, 258, 335
Tanaka, Y., & Shibazaki, N. 1996, ARA&A, 34, 607
Teraki, Y. et al. 2017, in prep
Torres, G., Andersen, J., & Giménez, A. 2010, A&ARv, 18, 67
Wang, X., & Wang, Z. 2014, ApJ, 788, 184
White, N. E., & van Paradijs, J. 1996, ApJ, 473, L25
Yuan, F., Gan, Z., Narayan, R., et al. 2015, ApJ, 804, 101

This paper has been typeset from a TEX/LATEX file prepared by the author.